THE JOURNAL OF BIOLOGICAL CHEMISTRY VOL. 287, NO. 36, pp. 30317–30327, August 31, 2012

Swedish Alzheimer Mutation Induces Mitochondrial Dysfunction Mediated by HSP60 Mislocalization of Amyloid Precursor Protein (APP) and Beta-Amyloid*

Received for publication, March 23, 2012, and in revised form, June 28, 2012 Published, JBC Papers in Press, June 29, 2012, DOI 10.1074/jbc.M112.365890

Ken Carlson Walls[‡§1], Pinar Coskun[‡§], Jose Luis Gallegos-Perez[‡], Nineli Zadourian[§], Kristine Freude[§], Suhail Rasool[¶], Mathew Blurton-Jones[‡§], Kim Nicholas Green[‡§], and Frank Michael LaFerla[‡§2]

From the [‡]Department of Neurobiology and Behavior, [§]Institute for Memory Impairments and Neurological Disorders, and the [¶]Department of Molecular Biology and Biochemistry, University of California, Irvine, California 92697-4545

Background: Alzheimer is associated with mitochondrial dysfunction, yet the mechanism leading to APP and beta-amyloid accumulation is unknown.
Results: Beta-amyloid and γ-secretase components accumulate in mitochondria via HSP60-mediated interactions.
Conclusion: HSP60 mediates accumulation of APP and beta-amyloid in the mitochondria of Alzheimer transgenic and human brains.
Significance: This study identifies a molecular player that translocates beta-amyloid and APP to mitochondria, contributing to its dysfunction.

Alzheimer disease (AD) is a complex disorder that involves numerous cellular and subcellular alterations including impairments in mitochondrial homeostasis. To better understand the role of mitochondrial dysfunction in the pathogenesis of AD, we analyzed brains from clinically well-characterized human subjects and from the 3xTg-AD mouse model of AD. We find Aβ and critical components of the γ-secretase complex, presenilin-1, -2, and nicastrin, accumulate in the mitochondria. We used a proteomics approach to identify binding partners and show that heat shock protein 60 (HSP60), a molecular chaperone localized to mitochondria and the plasma membrane, specifically associates with APP. We next generated stable neural cell lines expressing human wild-type or Swedish APP, and provide corroborating *in vitro* evidence that HSP60 mediates translocation of APP to the mitochondria. Viral-mediated shRNA knockdown of HSP60 attenuates APP and Aβ mislocalization to the mitochondria. Our findings identify a novel interaction between APP and HSP60, which accounts for its translocation to the mitochondria.

The etiology of Alzheimer disease (AD)[3] is not fully understood, though experimental evidence suggests mitochondrial impairment induced by enhanced reactive oxygen species (ROS) occurs early in the disease pathogenesis (1–3). Supporting mitochondria are a prominent organelle affected in AD are the studies in transgenic mouse models of AD that show altered mitochondrial bioenergetics arise prior to plaque development (4, 5). Amyloid beta (Aβ), the main component of plaques, accumulates in mitochondria collected from brains of human AD cases and transgenic mouse models of AD (6–8). Multiple studies investigating the role of Aβ in AD have directly linked Aβ to mitochondrial dysfunction by several possible mechanisms that include affecting cytochrome *c* oxidase of the respiratory chain, mitochondria membrane potential, ATP production, and fusion/fission interactions (9–11). Corroborating studies in cells lacking mitochondrial DNA have revealed Aβ-induced toxicity is dependent on a functional respiratory chain (12). The molecular processes that contribute to APP and Aβ mislocalization to the mitochondria in AD are undefined.

APP contains a mitochondrial target sequence, although its physiological function in the mitochondria remains unclear (13). APP is imported into this organelle through binding to the transporter outer membrane 40 (TOM40) and transporter inner membrane 23 (TIM23) mitochondrial import proteins, but complete translocation of APP to the mitochondria may be impeded by its acidic C-terminal sequence (13). To determine the effects of APP translocation to the mitochondria and its implication on mitochondrial function, previous investigation revealed that the γ-secretase complex that cleaves APP to generate Aβ was localized to the mitochondria (14). The mechanism responsible for APP and Aβ mitochondrial localization is undetermined; however, a recent study showed that rescuing activation of mitochondrial permeability pore complex via cyclopilin D deficiency attenuates Aβ-induced mitochondrial dysfunction and cognitive deficits. Consequently, these studies reveal mitochondria are a prominent organelle affected by Aβ (15).

Converging evidence from Parkinson disease (PD) and other neurological disorders show molecular chaperones play an integral role in neurodegeneration (16). Corroborating evidence implicates heat shock proteins (HSPs) in metabolism and the aggregation of both Aβ and tau (17, 18). Mitochondrial

* This work was supported, in whole or in part, by National Institutes of Health Grants 021928 and AG027544 awarded (to F. M. L.).
[1] To whom correspondence may be addressed: Department of Neurobiology and Behavior, University of California, Irvine CA 92697-4545. Tel.: 949-824-3471; Fax: 949-824-7356; E-mail: kwalls@uci.edu.
[2] To whom correspondence may be addressed: Department of Neurobiology and Behavior, University of California, Irvine, CA 92697-4545. Tel.: 949-824-3471; Fax: 949-824-7356; E-mail: laferla@uci.edu.
[3] The abbreviations used are: AD, Alzheimer disease; APP, amyloid precursor protein; Aβ, amyloid beta; HSP, heat shock protein; PD, Parkinson disease.

associated HSPs, mtHSP70/Grp75/Mortalin, HSP60, and HSP10, are predominantly found in the mitochondria matrix and play an important role in protein folding. Subcellular studies implicate HSP60 and mtHSP70 in many cellular functions by showing these chaperones localize to the plasma membrane, ER, and endocytic vesicles (19). Alterations in HSPs function cause pleiotropic effects on mitochondria function, such as protein aggregation, and import deficits leading to morphological changes (20). These studies connect HSPs in numerous cellular processes important for maintaining mitochondrial integrity.

In the present study, we sought to identify the molecular processes that contribute to APP and Aβ mislocalization to the mitochondria, and ultimately its dysfunction. Here we show 3xTg-AD mitochondria exhibit decreases in cox IV activity and respiratory capacity accompanied with increased Aβ and γ-secretase components. To identify the molecular determinants involved in APP and Aβ mislocalization to the mitochondria in the AD brain, we used a proteomics approach to identify APP and Aβ binding partners. We find HSP60 and APP/Aβ form a strong molecular association in mitochondria harvested from both transgenic and human AD subjects. Using a viral transduction strategy, we generated stable neural cell lines expressing human wild-type or Swedish APP, and provide substantiating *in vitro* evidence that HSP60 mediates translocation of APP to the mitochondria. Knockdown of HSP60 via an shRNA-based approach abrogated APP and Aβ localization to the mitochondria in Swedish APP-transduced cells. Our studies identify a novel interaction between APP and HSP60 that is important for its translocation to the mitochondria in AD.

EXPERIMENTAL PROCEDURES

3xTg-AD mice were previously characterized and maintained on a hybrid C57BL6/129 background (21). Female 12-month-old homozygous 3xTg-AD and age-matched hybrid controls were used for the purposes of these studies. All procedures were performed in accordance with the National Institutes of Health and University of California guidelines.

Human Tissue—Brain tissue collected by the University of California, Irvine Alzheimer Disease Research Center (ADRC) is tested for pathological hallmarks of AD. Human AD brains ($n = 8$) were processed as described below and compared with APOE allele-, age-, and sex-matched non-demented controls ($n = 8$). The average post mortem index for non-demented controls was 5.8 and 5.2 for AD specimens.

C17.2 Cells—Generation of these cells was described previously (22). C17.2 cells were passaged every other day by trypsinization and adding a tenth of the cells to a new flask.

Mitochondrial Fractionation—Mouse brains were submerged in 6 ml of mitochondrial homogenization buffer (H-Buffer) (225 mM mannitol, 75 mM sucrose, 10 mM MOPS, 1 mM EGTA, 0.5% BSA, pH 7.2, at 4 °C) followed by dounce homogenization on ice. Differential centrifugation was performed on homogenates followed by iodoxinal density gradient subcellular fractionation as performed previously (23). Collected fractions were washed in H-buffer and lysed in TBS with 2% CHAPs. Western blot analysis of GM130 (Golgi), calnexin (ER), GAPDH (cytosolic), and Complex IV subunit IV were assessed to determine the purity of each mitochondria preparation.

Complex Activity Assay—Complex IV activity was assessed from isolated mitochondrial preparations as described previously (2).

Respiration Assay—Respiration rates were determined by using the Clark-type electrode by Hansatech Oxygraph (Norfolk, England) instruments. Freshly prepared mitochondria, 500 μg of protein, was used to measure State 3 and 4 oxygen consumption rates in the presence of complex I substrate glutamate and malate. FCCP (*p*-trifluor-omethoxy carbonyl cyanide phenyl hydrazone) was used to measure uncoupling rate for the maximum respiration rate and oligomycin to inhibit Complex V.

DNP Derivative Assay—Oxyblot/DNP derivative assay (Millipore, Billerica, MA) was performed in accordance to the manufacturer's protocol.

ATP Assay—ATP levels were assessed using the manufacturer's protocol for the ATP lite activity assay (Perkin Elmer, San Jose, CA).

Seahorse XF-24 Extracellular Flux Analyzer—According to the manufacturer's protocol, four groups (APP_{WT}, APP_{SWE}, $APP_{WT}hsp60^{-/-}$, $APP_{SWE}hsp60^{-/-}$) of C17.2 cells plated in Seahorse XF-24 plates at a density of 6×10^4 cells/well, with 3 replicates/group were incubated overnight. After initial baseline measurements of OCR and ECAR, oligomycin (1 μM), *p*-trifluoromethoxy carbonyl cyanide phenyl hydrazone (FCCP at 1 μM) and Rotenone (1 μM)+ antimycine(1 μM) were sequentially injected to each wells for further OCR and ECAR determination. Total protein was determined from each well via Bio-Rad Bradford assay followed by protein normalization.

Cell Viability Assay—Cell viability assays were performed as described previously (24, 25).

ELISA—ELISA analysis was performed using beta-amyloid ELISA kits from WAKO (Wako catalogue #s 298-62401 and 294-62501). ELISA was performed on 100 μg of each mitochondrial lysates.

Western Blot—Western blots were preformed as described previously (25). Blots were probed for Cox IV, VDAC, Hsp60, and Cyt (Cell Signaling Technologies, Danvers, MA), 4G8 or 6E10 (Covance, Emeryville, CA), 22C11 (Millipore, Billerica, MA), GM130 (Abcam, San Francisco, CA), GAPDH (Santa Cruz Biotechnology, Santa Cruz, CA), serving as a loading control. Western blots were scanned into BioDoc (Bio-Rad) and quantified via imageJ.

Immunoprecipitation—Immunoprecipitation was performed using Dyna Beads (Invitrogen, Eugene, OR) as described by the manufacturer's protocol. Dyna beads were bound to 4G8, 6E10, or Hsp60. Antibody bound to dyna beads was incubated overnight with rotation in 400 μg of mitochondrial lysate or 800 μg of cytosolic lysate. Eluted proteins were then loaded on to a 4–12% gel followed by electrophoresis.

In-gel Tryptic Digest—Protein bands were excised and washed with 1:1 acetonitrile (ACN) and 50 mM ammonium bicarbonate (AMBC) and vortexed and incubated at 50 °C for 10 min for a total of three times. Gel pieces were dehydrated for 5 min with ACN and reduced with 10 mM DTT for 30 min. DTT was removed and iodoacetamide (100 mM) in AMBC and incu-

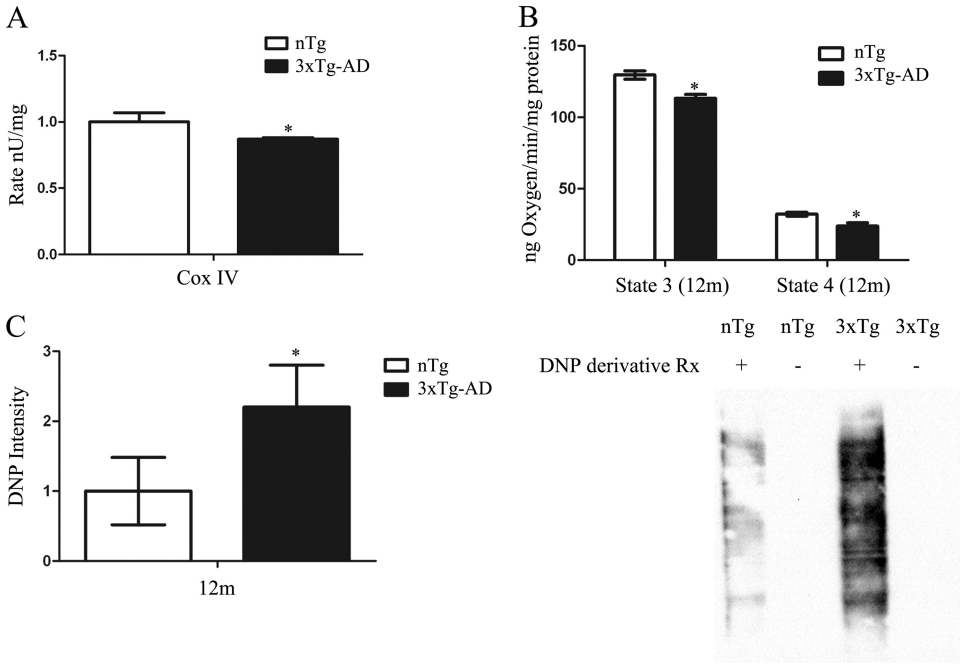

FIGURE 1. **3xTg-AD mitochondria exhibit deficits in oxidative phosphorylation and oxidative stress.** *A*, Cox IV activity was assessed by measuring the rate of oxidation of reduced cytochrome *c*. Cox IV was significantly decreased in 12-month-old 3xTg-AD compared with age-matched nTg ($n = 15$ for each time point from 3xTg-AD and nTg) (*B*) State 3 and state 4 respiration was determined by using mitochondria from cortical and hippocampal regions followed by oxygen electrode measurement in the presence of L-malate, L-glutamate, and ADP to initiate state 3 respiration and atractyloside to measure state 4. 3xTg-AD mitochondria exhibit a significant decrease in state 3 and 4 respiration compared with nTg ($n = 10$) (*C*) 5 μg of protein was subjected to the DNP conversion followed by Western blot analysis. DNP detection was significantly increased in 12-month-old 3xTg-AD mitochondria compared with age-matched controls. ($n = 6$ for each time point from 3xTg-AD and nTg). For all data points, *, $p < 0.05$ 3xTg-AD compared with nTg controls.

bated at room temperature for 30 min. Gel pieces were dehydrated with ACN for 5 min, removed, and 1× trypsin solution (Promega, Madison, WI) was added to the gel pieces. The following day, the supernatant was removed and 30 μl of extraction buffer (50% ACN and 5% formic acid in proteomic grade water) was added and removed every 10 min and placed into a new 1.5 ml tube. The concentrated peptides were desalted with zip tips (Millipore, Billerica, MA) and eluted in 10 μl of 50% (w/v) acetonitrile/0.1% trifluoroacetic acid.

Mass Spectrometry—To identify tryptic peptides matrix assisted laser desorption/ionization-time of flight (MALDI/TOF) mass spectrometry was performed. MS analysis was performed using a 5800 Plus MALDI TOF/TOF (Applied Biosystems, Framingham, MA) at the University of California, Irvine mass spectrometry core. The MS/MS spectra were analyzed using the Paragon algorithm (Protein Pilot software, Applied Biosystems, Carlsbad, CA) against the UniProt SP plus contaminant protein database. The search parameters were adjusted for cystein alkylation with idoacetamide. Additional parameters included a confidence interval $\geq$ 95% that was used for protein identification (Unused ProtScore > 1.3).

Lentiviral Vectors and RNAi—WT and Swedish (KM670/671NL) mutant APP lentiviral constructs were generated using the ViraPower^{TM} lentiviral expression system as described previously (26). Lentiviral shRNA HSP60 constructs were purchased from Sigma Aldrich. C17.2 cells underwent transduction as described previously (24).

Aβ Preparation—Aβ42 oligomers were prepared as described previously (27). Dot blot analysis confirmed Aβ42 oligomers, which tested negative for OC (fibril antibody) and positive for A11 (pre-fibrillar oligomers antibody).

Statistics—For experiments involving quantification, the standard error of the mean was determined from at least three independent experiments, with an "*n*" of one representing one transgenic mouse accompanied by one wild-type littermate control. Effects of genotype were analyzed for significance using two-way ANOVA, followed by Bonferroni's test for all pair-wise comparisons. In all cases, a p value of ≤ 0.05 was considered significant.

RESULTS

3xTg-AD Mice Exhibit Mitochondrial Deficits—Dysregulated mitochondrial function has been previously reported in the AD brain and various AD transgenic mouse models (4, 28). To elucidate the mechanism for mitochondrial dysfunction in AD, we used 12-month-old 3xTg-AD that have both Aβ and tau pathology (29). Complex IV activity, a critical component of the mitochondrial respiratory chain, was detected in either 3xTg-AD or non-transgenic (nTg) mitochondria by measuring the rate of oxidation of reduced cytochrome *c*. Complex IV activity was decreased in 3xTg-AD mitochondria compared with age-matched nTg (Fig. 1*A*). To test whether oxidative phosphorylation was impaired in 3xTg-AD mice, mitochondrial respiration was assessed from freshly isolated mitochondria from the forebrain. The respiratory rate was determined by adding mitochondrial substrates glutamate and malate (state 2), ADP (state 3), followed by oligomycin addition to inhibit complex IV (state 4). 3xTg-AD mitochondria showed decreases

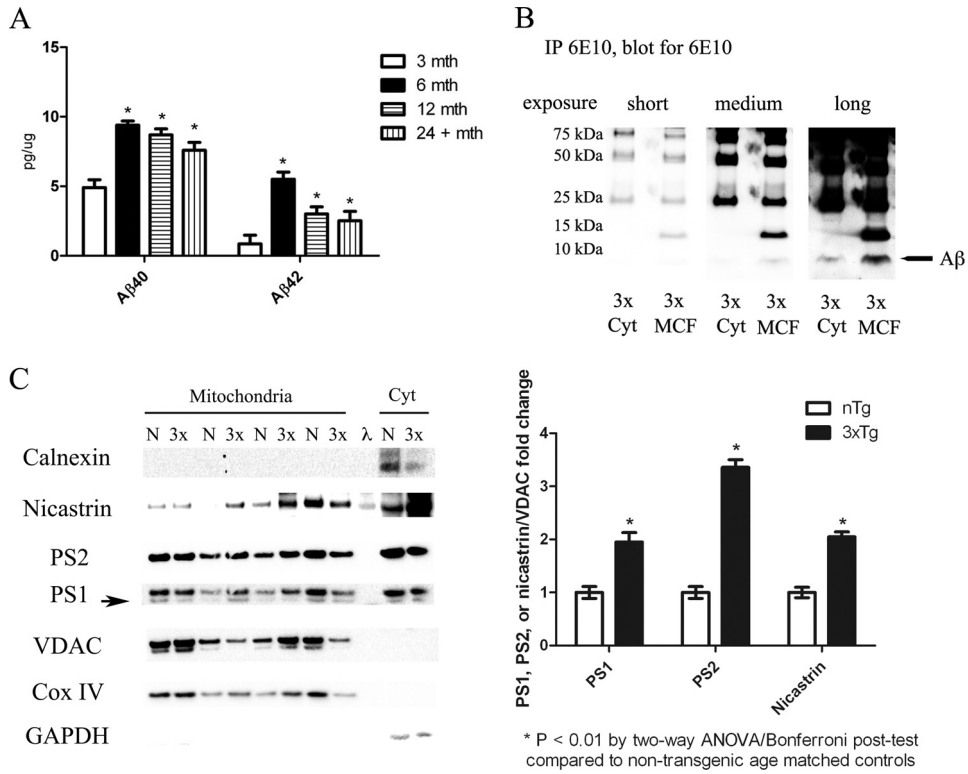

FIGURE 2. **3xTg-AD mitochondria exhibit increased Aβ and γ-secretase components.** *A*, Aβ40 (BA27) and Aβ42 (BC05) levels were examined via ELISA in 3xTg-AD mitochondrial fractions. Aβ40 and Aβ42 levels are significantly increased by 6 months of age and persist to 24 months compared with 3-month-old 3xTg-AD mitochondria. *B*, 6E10 was immunoprecipitated from either four pooled (100 μg each) 12-month 3xTg-AD cytosolic fractions or eight pooled mitochondrial containing fractions (MCF) followed by 6E10 -biotin immunoblot. Short, medium, and long exposure revealed increased Aβ monomer (4 kDa) in both 3$\times$ cytosolic and MCF fractions. Western blot analysis also showed an increase in an Aβ trimer at 12 kDa. *C*, Western blot analysis for PS1, PS2, nicastrin, VDAC, Cox IV, GAPDH, and calnexin was performed on 12-month-old 3xTg-AD and nTg mitochondrial fractions. λ represents the use of a ladder in the well. Results show increases in γ-secretase components compared with non-transgenic controls ($n = 8$). *, $p < 0.01$ by one-way ANOVA, 3xTg-AD γ-secretase protein levels *versus* nTg.

in respiration at both state 3 and 4 compared with nTg controls (Fig. 1*B*). Mitochondrial dysfunction is associated with both oxidative stress and AD related neuropathology. Consequently, to detect oxidative stress we employed the oxyblot detection system that converts oxidized side chains to 2,4-dinitrophenylhydrazone (DNP), which can be detected by Western blot. Mitochondria from 3xTg-AD revealed a significant increase in oxidative stress compared with nTg controls, as evidenced by increased DNP levels (Fig. 1*C*).

Increased Aβ and γ-Secretase Components in 3xTg-AD Mitochondria—To determine whether mitochondrial dysfunction was associated with increased Aβ localization to the mitochondria, differential centrifugation followed by density gradient fractionation was performed to obtain pure mitochondrial fractions (23). Biochemical analysis revealed mitochondrial fractions tested positive for mitochondrial proteins Complex IV subunit IV and VDAC, but negative for other organelle markers (*e.g.* calnexin and GM130) (Fig. 2*C* and data not shown). Western blot analysis on mitochondrial fractions showed no significant changes in APP levels in the 3xTg-AD mitochondria compared with non-transgenic controls, however, quantitative analysis by ELISA revealed $A\beta_{40}$ and $A\beta_{42}$ levels were significantly increased in 3xTg-AD mitochondria fractions at 6–24 months of age compared with non-pathological 3 month-old animals (Fig. 2*A* and data not shown). A recent study suggested 3xTg-AD mice have increased intraneuronal APP and not Aβ (30). To confirm our ELISA results 6E10 immunoprecipitation was performed on 12-month 3xTg-AD pooled cytosolic (400 μg) or mitochondrial containing fractions (800 μg). Western blot analysis to detect the Aβ monomer by using the 6E10 biotin conjugated antibody revealed increased Aβ monomer (4 kDa) in both 3xTg-AD cytosolic and mitochondrial containing fractions (Fig. 2*B*). Previous studies have shown that increased mitochondrial γ-secretase activity promotes Aβ generation by cleaving APP (14), which prompted us to investigate whether γ-secretase components were increased in the 3xTg-AD mitochondria. Corroborating with prior studies in AD transgenic mouse models, our Western blot results showed γ-secretase components presenilin-1, -2, and nicastrin were increased in 3xTg-AD mitochondria *versus* nTg controls (Fig. 2*C*), thus prompting further studies to investigate the mechanism responsible for Aβ accumulation in 3xTg-AD mitochondria.

APP/Aβ Species Interact with Molecular Chaperone HSP60—A proteomics approach to identify the mechanism responsible for APP and Aβ mislocalization to the mitochondria was performed on cytosolic and mitochondrial fractions to identify APP and Aβ binding proteins. Cytosolic and mitochondrial fractions were pooled from either 3xTg-AD or non-transgenic fractions and subjected to 4G8 (detects endogenous and exogenous APP/Aβ) immunoprecipitation, which showed many alterations between APP-binding proteins in 3xTg-AD com-

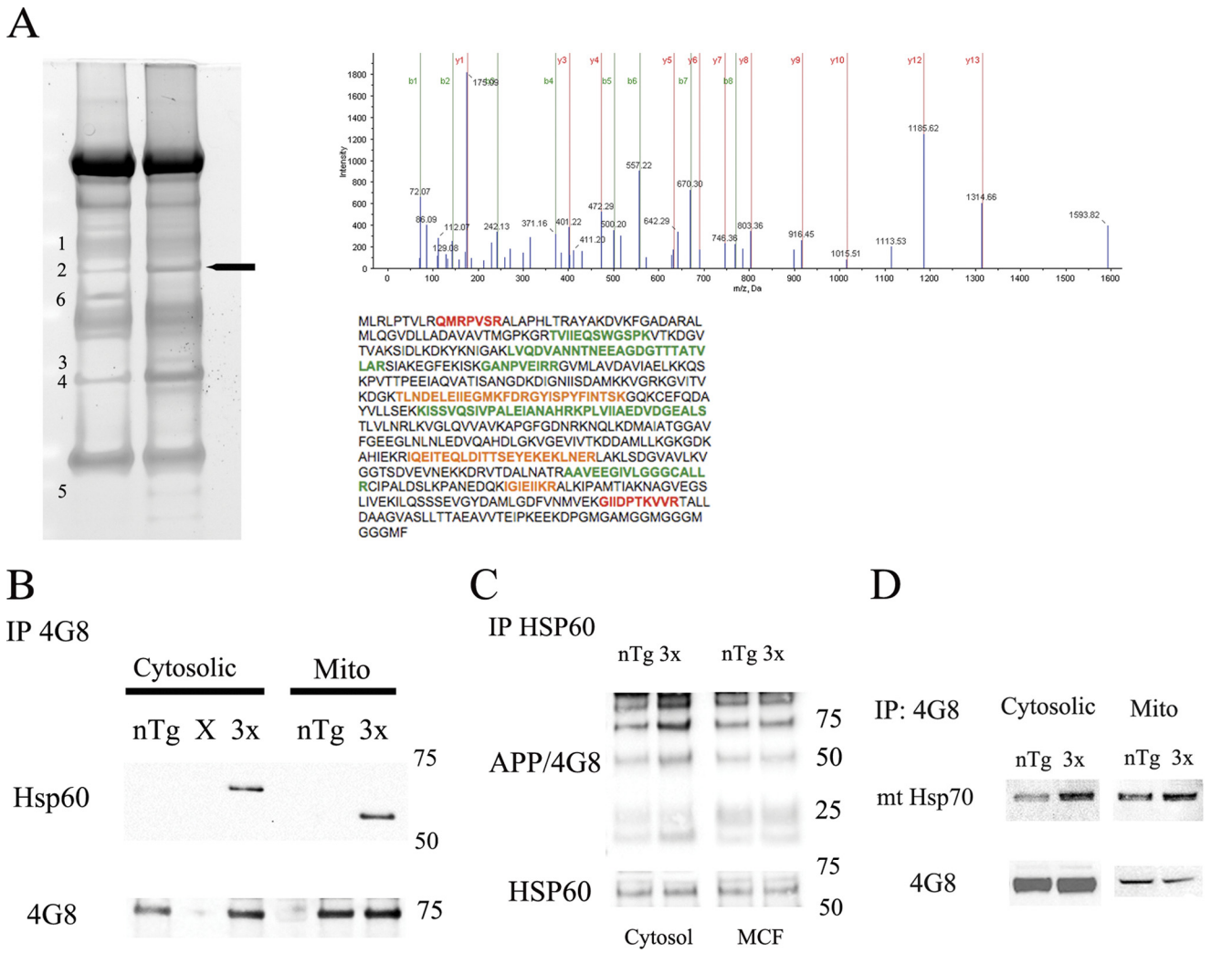

FIGURE 3. **3xTg-AD exhibit increased interactions between mitochondrial chaperone proteins and APP/Aβ.** *A*, APP/Aβ IP (4G8) was performed on 800 μg of cytosolic fractions pooled from either 4 non-transgenic (*left lane*) or 4 3xTg-AD (*right lane*) 12-month-old samples. A band approximately at 60 kDa was excised and processed for mass spectrometry. The band was identified as HSP60, which is represented by the MS/MS spectra from a peptide sequence with over a 99% confidence level. The HSP60 peptide sequence with peptides identified with high (*green text*) to moderate (*orange text*) confidence. Additional proteins identified, GAPDH, dihydropyrimidenase-2, isocitrate dehydrogenase (spot 1), heat shock protein 60 (2), isocitrate dehydrogenase (3), GAPDH (4), myelin basic protein isoform (5), and tubulin (6). *B*, co-IP experimentation by pulling down APP/Aβ (4G8) and blotting for HSP60 revealed increased APP/Aβ binding to HSP60 in both cytosolic and mitochondrial fractions pooled from 4 3xTg-AD age matched samples compared with 4-pooled non-transgenic samples. 4G8 immunoblot showed equal levels of APP/Aβ were pulled down. *C*, HSP60 IP followed by 4G8 immunoblot shows increased APP binding to HSP60 in 12-month 3xTg-AD cytosolic fractions compared with nTg controls. HSP60 immunoblot shows equal amounts of HSP60 were immunoprecipitated. *D*, co-IP experimentation by pulling down APP/Aβ (4G8) and blotting for mtHSP70 revealed a slight increase in APP/Aβ binding to mtHSP70 in the cytosolic, but not mitochondrial fraction pooled from 4-pooled 3xTg-AD age-matched samples compared with four pooled non-transgenic samples. 4G8 immunoblot showed equal levels of APP/Aβ were pulled down.

pared with non-transgenic that were analyzed by mass spectrometry (MS) (Fig. 3*A*). To identify potential proteins that could assist in APP/Aβ mitochondria translocation, gel bands were excised followed by in-gel tryptic digestion and MS. Of the proteins identified by matrix assisted laser desorption ionization time of flight (MALDI-TOF) MS/MS, HSP60 underwent further investigation based on previous results implicating it as an important mitochondrial chaperone. To confirm our MS results, Co-IP analysis was performed on pooled cytosolic and mitochondria fractions from either non-transgenic or 3x-Tg-AD mice. APP/Aβ (4G8) immunoprecipitation followed by HSP60 immunoblot revealed APP and/or Aβ binding was increased in the 3xTg-AD brain and virtually undetectable in non-transgenic animals (Fig. 3*B*). It is noteworthy that HSP60 undergoes post-translational modification upon mitochondrial import, including the removal of 27 amino acids (31). In addition, mtHSP70, another mitochondrial chaperone interaction was assessed, however the interaction was not as pronounced as the APP/HSP60 interaction (Fig. 3*D*). To verify the interaction, immunoprecipitation of HSP60 followed by 4G8 detection was performed. Western blot analysis revealed increased APP binding to HSP60 in the 3xTg-AD cytosolic and mitochondrial fractions compared with non-transgenic controls (Fig. 3*C*). These results reveal increased interactions between mitochondrial chaperone HSP60 and APP in 3xTg-AD.

HSP60 and APP Interaction Exists in Human AD—Tissue collected by the University of California, Irvine Alzheimer Disease Research Center (ADRC) undergoes rigorous cognitive and pathological analysis to validate AD *versus* non-demented specimens. To determine whether Aβ accumulates in mito-

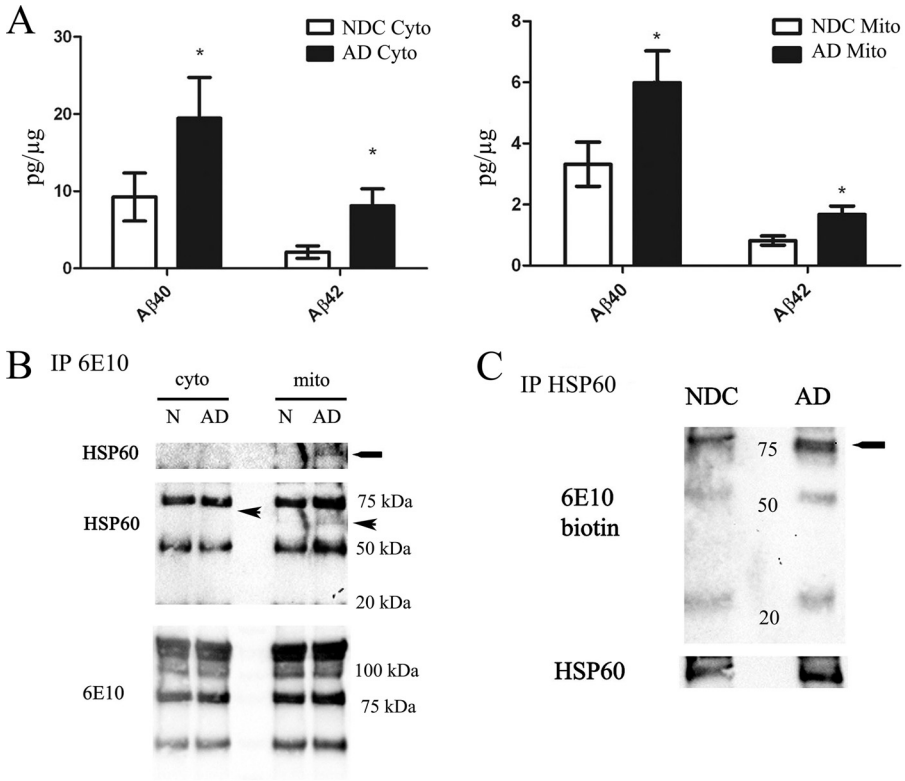

FIGURE 4. **The interaction between APP and HSP60 exists in the human brain.** *A*, ELISA analysis showed increased Aβ40/42 in AD brains compared with normal controls, $n = 4$ for both AD and non-demented controls. *, $p < 0.001$ AD mitochondria compared with Normal controls. *B*, 6E10 was immunoprecipitated from either pooled cytosolic ($n = 8$) or mitochondrial fractions ($n = 8$) followed by HSP60 immunoblot. The HSP60 interaction between APP/Aβ was slightly detectable in AD pooled mitochondrial fractions compared with NDC controls. The *arrow* represents the anticipated molecular weight of HSP60 in the cytosol. *C*, to confirm the interaction between APP/Aβ and HSP60, HSP60 immunoprecipitation was performed on 8 pooled NDC or AD mitochondrial containing fractions (800 μg total) followed by 6E10 biotin Western blot. APP doublet (~75 kDa) binding to HSPs was observed in AD mitochondria compared with NDC. *D*, 4G8 was immunoprecipitated from either pooled cytosolic ($n = 4$) or mitochondrial fractions ($n = 8$) followed by mtHsp70 immunoblot. The mtHsp70 interaction between APP and its derivatives was slightly increased in 3xTg samples compared with nTg controls.

chondria from AD subjects *versus* normal, non-demented controls, mitochondrial fractions were prepared followed by biochemical analysis. Our ELISA results showed significant increases in both Aβ40 and Aβ42 in both the AD cytosolic and mitochondrial fractions compared with non-demented controls (Fig. 4*A*). To test whether HSP60 interacted with APP and/or Aβ occurred in the AD brain, pooled cytosolic or mitochondrial fractions from either AD or non-demented controls were subjected to immunoprecipitation with 6E10 (human specific antibody for APP/Aβ) followed by HSP60 immunoblotting. We found AD mitochondria exhibit increased HSP60 binding to APP/Aβ compared with non-demented controls (Fig. 4*B*). HSP60 was undetectable in the cytosolic fraction pull down (Fig. 4*B*). To verify these results, immunoprecipitation of HSP60 was performed from 8 pooled human mitochondrial containing fractions followed by Western blotting with the 6E10 antibody conjugated to biotin to avoid detection of heavy and light chains. Our results revealed increases in HSP60 binding to APP in the AD mitochondria in contrast to non-demented controls (Fig. 4*C*).

Swedish APP Leads to Aβ-induced Mitochondrial Dysfunction—To better understand the molecular process associated with Aβ intracellular accumulation, a neural cell line (C17.2) was transduced with lentiviruses containing either wild-type human APP (APP_{WT}) or familial AD Swedish mutation (APP_{SWE}) that causes BACE cleavage, thus generating more Aβ. To delineate the influence of the Swedish mutation on APP and Aβ mitochondrial translocation, cytosolic lysates, whole cell lysates, and mitochondrial-containing fractions were prepared from either APP_{WT} or APP_{SWE} cells. Western blot analysis on either cytosolic or whole cell lysates showed no significant increases in total APP protein levels between APP_{WT} and APP_{SWE} (Fig. 5*A* and data not shown). Mitochondrial fractions from the APP_{SWE} mutation showed a significant increase in APP and its derivatives in comparison to APP_{WT} (Fig. 5*A*). To verify the purity of the fractions, VDAC and Complex IV Subunit IV were used to quantify mitochondrial fractions, while β-tubulin was used as a cytosolic loading control. To determine whether oxidative phosphorylation was compromised in APP_{SWE} *versus* APP_{WT}, an ATP luciferase activity assay was performed on both cell lines and revealed APP_{SWE} cells produced significantly less ATP production compared with APP_{WT} cells (Fig. 5*B*). To further assess mitochondrial respiration, APP_{WT} and APP_{SWE} lines were treated with antimycin (inhibits flow of electrons from cytochrome *b* to cytochrome c_1, complex III), oligomycin (inhibits ATP synthase by blocking its proton channel (Fo subunit), and carbonyl cyanide *m*-chloro phenyl hydrazone (CCCP, uncoupler). ATP luciferase activity showed APP_{SWE} cells were significantly more susceptible to mitochondrial inhibitors and uncouplers *versus* APP_{WT} cells. APP_{SWE} cells also exhibited a slight increase in oxidative stress compared with APP_{WT} cells as evidenced by the DNP deriva-

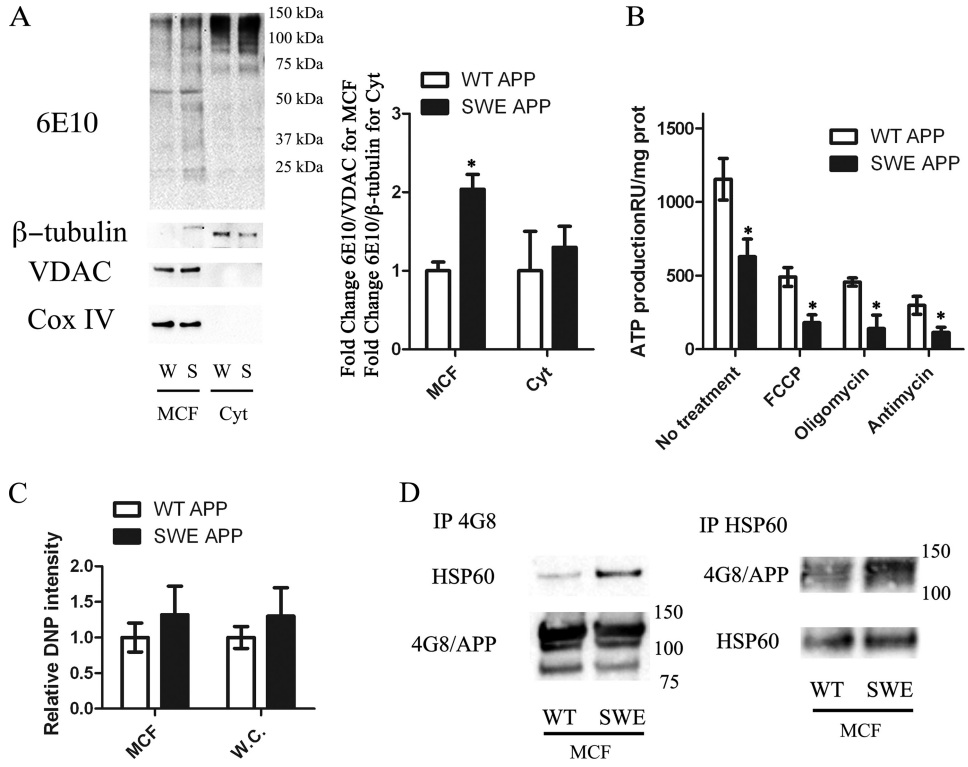

FIGURE 5. ***In vitro* FAD mutation promotes APP/Aβ mitochondrial accumulation and mitochondrial dysfunction.** *A*, mitochondrial containing and cytosolic fractions were prepared and blotted for mitochondrial markers Cox IV and VDAC, while β-tubulin was used to verify cytosolic fractions. Western blot analysis for human APP (6E10) revealed a significant increase in APP/Aβ derivatives in SWE (*S*) mitochondrial fractions compared with WT APP (*W*). *B*, ATP levels were assessed with an ATP luciferase assay in both W and S cell lines. ATP production was significantly decreased in the SWE cell line compared with WT. In addition, SWE cells were more sensitive to mitochondrial uncoupler (FCCP), complex III inhibitor (antimycin), and the ATP synthase inhibitor oligomycin compared with WT. *C*, 5 μg of protein from either WT or SWE whole cell lysates and MCF fractions were subjected to the DNP derivative assay followed by Western blotting. SWE cells exhibited increased DNP activity compared with WT cells ($n = 8$). All data points, *, $p < 0.05$ SWE cells compared with WT APP cells. *D*, co-IP experimentation by pulling down APP/Aβ (4G8) and blotting for HSP60 showed increases in APP/Aβ binding to HSP60 in APP_{SWE} mitochondrial-containing fractions (*MCF*) compared with APP_{WT} ($n = 6$). HSP60 IP followed by 4G8 immunoblot shows increased APP binding to HSP60 in APP_{SWE} cells compared with APP_{WT}. 4G8 and HSP60 immunoblots show equal amounts of HSP60 and 4G8 were immunoprecipitated for each experiment.

tive assay (Fig. 5*C*). To determine whether the APP_{SWE} mutant resulted in increased APP binding to HSP60, immunoprecipitation using 4G8 was performed on pooled mitochondrial-containing fractions ($n = 6$ for each group). Western blot analysis revealed APP_{SWE} cells exhibit increased APP binding to HSP60 in contrast to APP_{WT} (Fig. 5*D*). To verify these results, immunoprecipitation using HSP60 was conducted on pooled mitochondrial containing fractions followed by Western blotting with 4G8 antibody. Our results corroborated our *in vivo* results showing increased HSP60 binding to APP in the AD mitochondria.

HSP60 Mediates APP and Aβ Localization to the Mitochondria—To determine the role HSP60 plays in APP and Aβ mitochondrial translocation and its effects on mitochondrial homeostasis, lentiviruses containing either HSP60 shRNA or PLKO (empty control vector) were generated in APP_{WT} and APP_{SWE} cell lines. Western blot analysis revealed HSP60 levels were drastically reduced by shRNAs directed toward HSP60 compared with PLKO controls (Fig. 6*A*). To test the hypothesis that HSP60 is important for APP and Aβ mislocalization to the mitochondria, mitochondrial fractions were prepared from APP_{WT} and APP_{SWE} cells with or without HSP60 knockdown. Biochemical analysis showed the increased Aβ and APP in the Swedish mitochondria fraction was significantly reduced by HSP60 knockdown compared with cells expressing the Swedish mutation and PLKO (Fig. 6*A*). HSP60 knockdown had no effect on APP and its derivatives in the APP_{WT} mitochondrial fractions. To determine whether Aβ levels were diminished in the HSP60 knockdown lines, ELISA analysis was performed to detect $A\beta_{40}$ and $A\beta_{42}$ levels. Our results showed that APP_{SWE} cells have significant increases in mitochondrial $A\beta_{40}$ and $A\beta_{42}$ compared with APP_{WT}, and that HSP60 knockdown attenuated Swedish-induced mitochondrial Aβ accumulation (Fig. 6*B*).

To assess whether HSP60 knockdown could revert diminished ATP levels back to APP_{WT} levels, an ATP luciferase assay was performed on APP_{WT} and APP_{SWE} with or without HSP60. Our results showed HSP60 knockdown did not ameliorate the diminished ATP levels observed in APP_{SWE} cells (Fig. 7*A*). HSP60 knockdown decreased ATP production in WT_{APP} cells, corroborating with previous findings the importance of HSP60 in mitochondrial bioenergetics. To further assess the impact of HSP60 knockdown on mitochondrial function, basal cellular respiration and glycolysis were determined in APP_{WT} and APP_{SWE} with or without HSP60 by using the Seahorse XF-24 metabolic flux analyzer. Oxygen consumption rates (OCR) and extracellular acidification rates (ECAR) were calculated. Basal respiration was established followed by the addition of 1 μm oligomcyin (vertical line A), which showed a decline in OCR by ~50%, revealing oxygen consumption in these cells utilizes

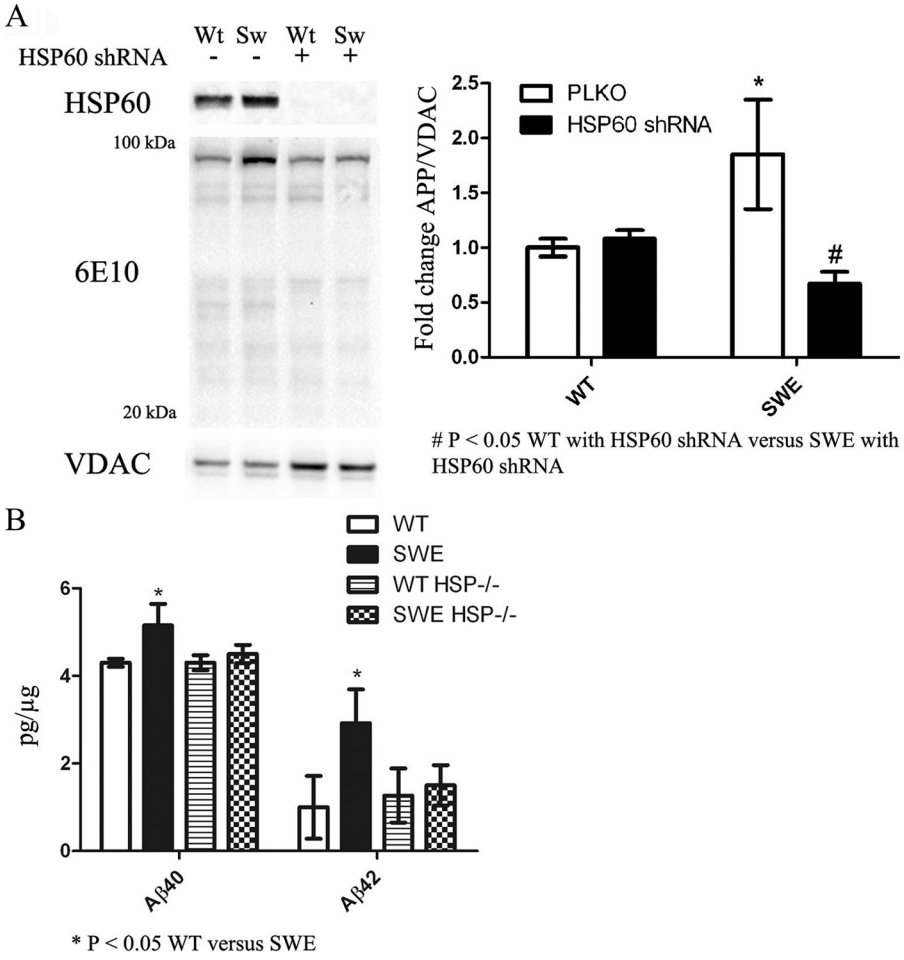

FIGURE 6. **HSP60 knockdown attenuates SWE-induced APP/Aβ mitochondrial translocation.** *A*, lentiviruses containing HSP60 shRNA (clones 95, 96, and 99) were generated followed by neural cell transduction. Western blot analysis shows dramatic reduction of HSP60 levels in all three clones. β-Tubulin was used as a loading control. Mitochondrial fractions were prepared from WT or SWE lines with or without HSP60 shRNA followed by Western blot analysis to assess APP/Aβ levels. Increased APP levels in the SWE expressing cell line were returned to WT levels with HSP60 knockdown. *B*, ELISA analysis performed on mitochondrial fractions showed that the increased Aβ levels in SWE-expressing cells were returned to baseline with HSP60 knockdown. *, $p < 0.05$ by two-way ANOVA/Bonferroni post-test compared with WT.

both oxidative phosphorylation and glycolysis equally (Fig. 7, *B* and *C*). Additionally APP_{SWE} cells exhibit a higher maximal respiratory capacity rate than APP_{WT} cells, whereas, HSP60 knockdown in both APP_{WT} and APP_{SWE} significantly diminished the maximal respiratory rate (Fig. 7*B*). We also found the Swedish mutation induced Aβ that diminishes ATP levels causes a compensatory mechanism by increasing maximal respiration (Fig. 7*B*). Furthermore, to determine whether HSP60 knockdown could attenuate a secondary insult, we treated APP_{WT} and APP_{SWE} cells with or without HSP60 knockdown with Aβ oligomers for 48 h. Viability analysis showed APP_{SWE} cells were more susceptible to Aβ oligomer-induced cell death compared with APP_{WT}, however, HSP60 knockdown cells were just as vulnerable to Aβ oligomer-induced cell death in both APP_{WT} and APP_{SWE} cells (Fig. 7*D*). In addition to its role in maintaining mitochondrial homeostasis, we show HSP60 also mediates APP and Aβ mislocalization to the mitochondria.

DISCUSSION

In the present study, we sought to identify the molecular processes that contribute to APP and Aβ mislocalization to the mitochondria, and ultimately its dysfunction. Here we demonstrate that mitochondria harvested from 3xTg-AD mice are impaired, as evidenced by decreases in state 3 and 4 respiration, lower cox IV activity, and elevated oxidative stress. Our study further shows that 3xTg-AD mitochondria exhibit increased Aβ and γ-secretase components, providing a platform to investigate the mechanism responsible for APP and Aβ ectopic localization to the mitochondria. To identify the molecular determinants involved in APP and Aβ localization to the mitochondria in the AD brain, we used a proteomics approach to identify APP and Aβ binding partners. Proteomic and biochemical analyses of 3xTg-AD mitochondria identified a novel interaction between APP and HSP60. We found HSP60 and APP/Aβ form a strong molecular association in mitochondria from both transgenic and human AD subjects. APP immunoprecipitated from human AD mitochondria exhibited a stronger propensity to interact with HSP60 *versus* non-demented controls. Using a viral transduction approach, we generated stable neural cell lines expressing either human wild-type APP or Swedish APP, and provided substantiating *in vitro* evidence that HSP60 forms a strong molecular association with APP in

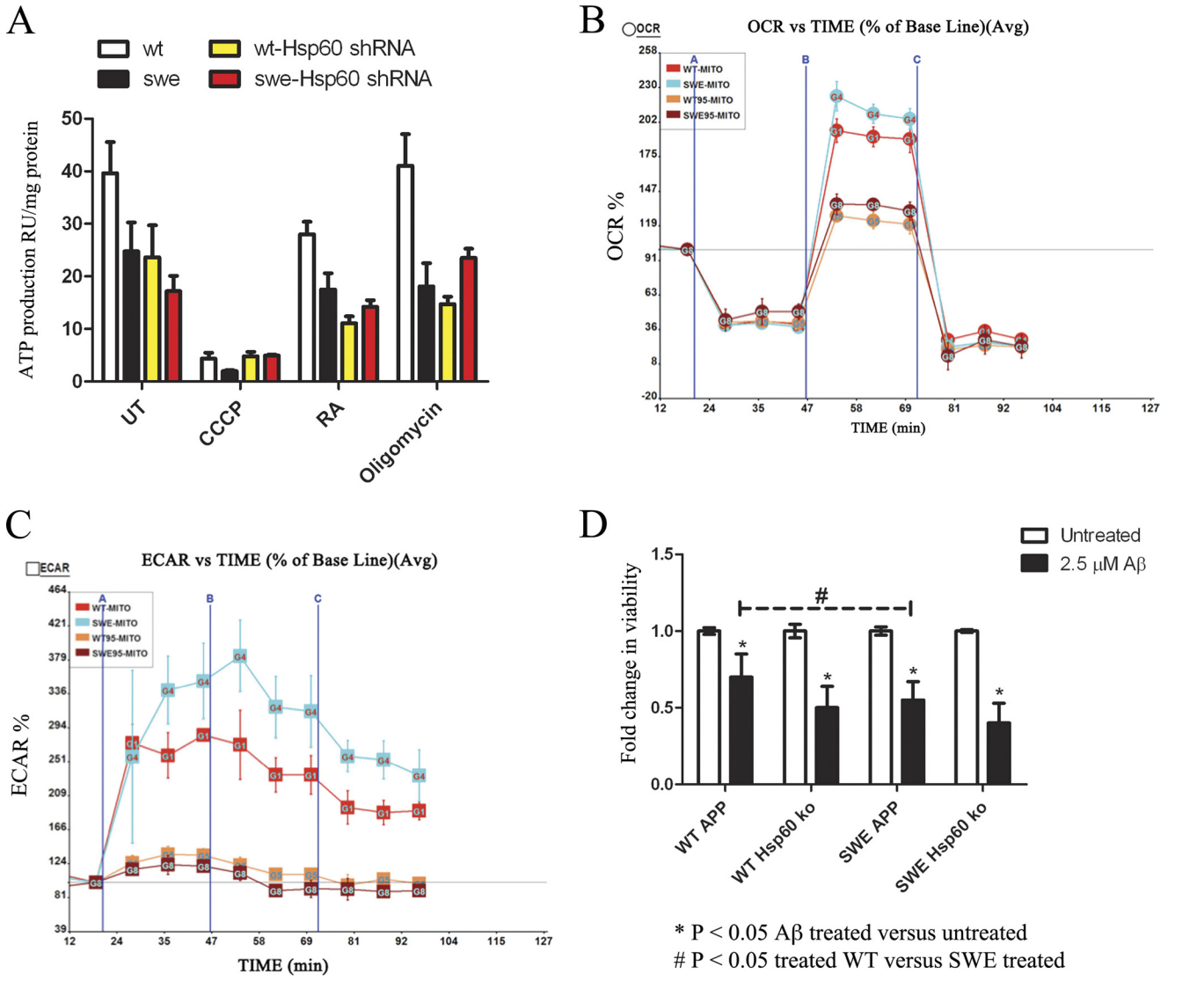

FIGURE 7. **Mitochondrial homeostasis requires HSP60.** *A*, ATP levels were assessed with an ATP luciferase assay in both WT and SWE cells with or without HSP60 knockdown. ATP production was decreased in the SWE cells compared with WT and both WT- and SWE-HSP60 shRNA-transduced cells. SWE-HSP60 shRNA cells were less sensitive to ATP synthase inhibitor oligomycin, however, HSP60 knockdown had no effect on ATP levels when treated with FCCP, rotenone, and antimycin (*RA*). *B*, OCR determined by Seahorse XF-24 Metabolic flux analyzer showed APP_{SWE} cells have slight increases in proton leakage and maximal respiration that is attenuated with HSP60 knockdown. *Vertical lines* indicate time of addition of mitochondrial inhibitors oligomycin (1 μm, *A*), FCCP (1 μm, *B*), or rotenone (1 μm, *C*). Bars represent percent change in OCR from baseline ± S.E. (*, $p < .05$). *C*, ECAR analysis reveals APP_{SWE} cells utilize glycolysis compared with WT, which is inhibited by HSP60 knockdown. Bars represent percent change in OCR from baseline ± S.E. (*, $p < 0.05$) (*D*) WT or SWE cells with or without HSP60 knockdown were treated with 2.5 μM $A\beta_{1-42}$ oligomers for 48 h followed by viability analysis. SWE cells were significantly more susceptible to Aβ-induced death compared with WT cells. HSP60 knockdown showed neither protection or exacerbation of Aβ-induced neural cell death. *, $p < 0.05$ by two-way ANOVA/Bonferroni post-test compared with WT.

an *in vitro* model of familial AD. Knockdown of HSP60 abrogated APP and Aβ localization to the mitochondria in Swedish APP-expressing cells. This study identifies a novel interaction between APP and HSP60 that is important for APP and Aβ translocation to the mitochondria.

Biochemical analysis of 3xTg-AD showed Aβ and γ-secretase components accumulated in mitochondrial fractions, corroborating previous studies that found Aβ and APP localized to the mitochondria leading to its dysfunction. 6E10 immunoprecipitation identified Aβ monomers accumulating in 3xTg-AD cytosol and mitochondria, whereas, a ~12 kDa band was also detected in the mitochondrial fraction that was not apparent in the cytosolic fraction. The ~12 kDa band likely represents an Aβ trimer or C99, that could potentially disrupt mitochondrial function. A recent study found mitochondria from 5XFAD mice accumulate the C99 fragment, resulting in mitochondrial dysfunction (32); consequently, APP mitochondrial localization takes on added significance, since our findings and others have detected increased mitochondrial Aβ and γ-secretase components in AD patients (14). To determine the mechanism responsible for APP and Aβ mislocalization to the mitochondria, neural cells expressing human wild-type APP or Swedish APP were generated and provided supporting *in vitro* evidence that APP and Aβ accumulate in the mitochondrial concomitant with decreased ATP levels and elevated oxidative stress. 3xTg-AD mice harbor the APP_{SWE} mutation, which promotes $A\beta_{42}$ generation. This explains why we did not observe significant changes in total APP protein levels between the human

wild-type and Swedish APP whole cell lysates. However, we did detect increased APP and Aβ in the mitochondria of APP_{SWE} cells *versus* APP_{WT}. These results indicate that the familial AD Swedish mutation generates more $A\beta_{42}$ and induces mitochondrial dysfunction. Corroborating previous reports that showed APP_{SWE} cells were healthy (33), this was justified by cellular respiration analysis that demonstrated both APP_{SWE} and APP_{WT} cells utilize oxidative phosphorylation and glycolysis equally, thus providing an alternate energy source if oxidative phosphorylation is compromised. Unexpectedly, respiration results revealed that the maximal respiration was increased in APP_{SWE} cells, suggesting APP_{SWE} cells compensate for diminished ATP levels. APP_{SWE}-expressing cells also exhibited elevated, but not significant levels of oxidative stress, most likely due to the ability of pre-mitotic C17.2 cells to dilute out reactive oxygen species with each cell division in contrast to post-mitotic neurons. We did find that APP_{SWE} cells were more susceptible to a secondary insult, such as Aβ oligomers. These results add to previous findings that APP and Aβ ectopic localization to the mitochondria cause its dysfunction.

To determine the molecular process involved in APP and Aβ localization to the mitochondria in 3xTg-AD mice, a proteomic strategy was performed identifying HSP60 as an APP/Aβ binding partner. Immunoprecipitation with either 4G8 or 6E10 showed HSP60 forms a strong interaction with APP in both cytosolic and mitochondrial fractions from 3xTg-AD and cells expressing Swedish APP compared with controls. Although HSP60 immunoprecipitation exhibited only a slight increase in the APP/HSP60 interaction in either fraction, these results imply that the rabbit polyclonal HSP60 antibody nonspecifically binds to additional proteins in the fraction that share sequence homology with APP, such as amyloid-like protein 1 or APLP1 or APLP2. APLP1 and APLP2 are similar to APP except they lack the Aβ domain. APLP2 is a more likely candidate at the mitochondria than APLP1 based on subcellular studies showing APLP2 is predominantly intracellular, whereas APLP1 is associated with the plasma membrane (34). The HSP60/APP interaction is stronger with 4G8 and 6E10 antibodies, because these are monoclonal antibodies that target the Aβ epitope. Immunoprecipitation of HSP60 or APP showed APP complexes with HSP60 in AD mitochondria *versus* non-demented controls. In contrast to 3xTg-AD, the cytosolic interaction was undetectable in both human AD and non-demented controls, proposing cytosolic HSP60 is rapidly degraded by active proteases, since human brains were not subjected to the same rapid freezing protocol performed on mouse brains. This likely scenario proposes mitochondrial HSP60 is in part protected from degradation, since it is compartmentalized in the mitochondria, although mitochondria also possess proteases, thus making the interaction less robust compared with our *in vivo* and *in vitro* results. These findings are significant in that they reveal increased binding of HSP60 to APP in the AD brain.

Combining *in vivo* and *in vitro* models of AD, we have demonstrated the interaction between HSP60 and APP is increased in the AD brain. To determine the mechanism responsible for APP and Aβ localization to the mitochondria, neural cells expressing the Swedish APP mutation that produces more Aβ and leads to mitochondria dysfunction were used to discern whether HSP60 mediated APP and Aβ localization to this organelle. Knockdown of HSP60 by shRNA attenuated ectopic localization of APP and Aβ to the mitochondria in Swedish APP expressing cells. Human wild-type APP expressing cells were unaffected by HSP60 knockdown, supporting our hypothesis that Aβ induces HSP60-mediated mislocalization of APP and Aβ to the mitochondria. Chaperone interactions are stimulus specific, thus alterations in cellular homeostasis may free the chaperone to associate with additional substrates. HSP60 has been implicated in possessing both anti- and pro-apoptotic roles (35). Under normal physiological conditions HSP60 forms a pro-survival complex with Bcl-2, an anti-apoptotic mediator, and this complex is hindered by nutrient deprivation resulting in cell death (33). Consequently, increases in Aβ may interact with HSP60 directly or indirectly to release HSP60 from Bcl-2, thus freeing HSP60 to mediate APP and Aβ mislocalization to the mitochondria and promote mitochondrial dysfunction. This hypothesis coincides with previous findings that show HSP60 possess pro-apoptotic abilities by initiating the maturation of procaspase-3 to promote apoptosis (36). To test whether HSP60 knockdown would be protective in response to Aβ-induced mitochondrial dysfunction, we treated HSP60 knockdown cells with Aβ oligomers, and found HSP60 knockdown cells offered no significant protection. One such explanation is Aβ oligomers cause Bcl-2 to be sequestered by pro-apoptotic Bcl-2 homology 3 domain (BH3) proteins, which bind and suppress Bcl-2 pro-survival function in the absence of HSP60. Accordingly, Bcl-2 would be more prone to inhibitory mechanisms without HSP60, thus corroborating with previous reports that show HSPs are important for maintaining cellular homeostasis. Earlier studies revealed Aβ binds and inactivates complex IV of the respiratory chain (37); therefore, Aβ and APP binding to HSP60 may disrupt its physiological role at the mitochondria leading to the organelles malfunction. Supporting that HSP60 is important for mitochondrial bioenergetics is our findings that HSP60 knockdown caused a greater deficiency in mitochondrial function as evidenced by decreased ATP and respiration. These results indicate that the familial AD Swedish mutation generates more $A\beta_{42}$ and induces mitochondrial dysfunction by promoting HSP60-mediated APP/Aβ mislocalization.

In conclusion, previous reports have identified mitochondrial proteins that promote import of APP and Aβ into the mitochondria; however, very little is known to what mediates APP and Aβ localization to the mitochondria during pathological conditions. Our results provide evidence that Aβ induces HSP60-mediated APP/Aβ mislocalization to the mitochondria, ultimately leading to its dysfunction. This finding is significant based on previous studies implicating APP and Aβ mitochondria accumulation in the buildup of oxidative stress, and eventually leads to mitochondrial dysfunction. In conclusion, our findings provide insight into the mechanism behind APP and Aβ mislocalization to the mitochondria that contributes to mitochondrial dysfunction.

REFERENCES

1. Reddy, P. H., and Beal, M. F. (2005) Are mitochondria critical in the pathogenesis of Alzheimer's disease? *Brain Res. Brain Res. Rev.* **49,** 618–632

2. Coskun, P., Wyrembak, J., Schriner, S., Chen, H. W., Marciniack, C., Laferla, F., and Wallace, D. C. (2011) A mitochondrial etiology of Alzheimer and Parkinson disease. *Biochim. Biophys. Acta* **1820,** 553–564
3. Swerdlow, R. H. (2007) Pathogenesis of Alzheimer's disease. *Clin. Interv. Aging* **2,** 347–359
4. Yao, J., Irwin, R. W., Zhao, L., Nilsen, J., Hamilton, R. T., and Brinton, R. D. (2009) Mitochondrial bioenergetic deficit precedes Alzheimer's pathology in female mouse model of Alzheimer's disease. *Proc. Natl. Acad. Sci. U.S.A.* **106,** 14670–14675
5. Takuma, K., Yao, J., Huang, J., Xu, H., Chen, X., Luddy, J., Trillat, A. C., Stern, D. M., Arancio, O., and Yan, S. S. (2005) ABAD enhances Aβ-induced cell stress via mitochondrial dysfunction. *FASEB J.* **19,** 597–598
6. Manczak, M., Anekonda, T. S., Henson, E., Park, B. S., Quinn, J., and Reddy, P. H. (2006) Mitochondria are a direct site of Aβ accumulation in Alzheimer's disease neurons: implications for free radical generation and oxidative damage in disease progression. *Hum. Mol. Genet.* **15,** 1437–1449
7. Caspersen, C., Wang, N., Yao, J., Sosunov, A., Chen, X., Lustbader, J. W., Xu, H. W., Stern, D., McKhann, G., and Yan, S. D. (2005) Mitochondrial Aβ: a potential focal point for neuronal metabolic dysfunction in Alzheimer's disease. *FASEB J.* **19,** 2040–2041
8. Gillardon, F., Rist, W., Kussmaul, L., Vogel, J., Berg, M., Danzer, K., Kraut, N., and Hengerer, B. (2007) Proteomic and functional alterations in brain mitochondria from Tg2576 mice occur before amyloid plaque deposition. *Proteomics* **7,** 605–616
9. Cardoso, S. M., Santana, I., Swerdlow, R. H., and Oliveira, C. R. (2004) Mitochondria dysfunction of Alzheimer's disease cybrids enhances Aβ toxicity. *J. Neurochem.* **89,** 1417–1426
10. Swerdlow, R. H., and Kish, S. J. (2002) Mitochondria in Alzheimer's disease. *Int. Rev. Neurobiol.* **53,** 341–385
11. Wang, X., Su, B., Siedlak, S. L., Moreira, P. I., Fujioka, H., Wang, Y., Casadesus, G., and Zhu, X. (2008) Amyloid-β overproduction causes abnormal mitochondrial dynamics via differential modulation of mitochondrial fission/fusion proteins. *Proc. Natl. Acad. Sci. U.S.A.* **105,** 19318–19323
12. Cardoso, S. M., Santos, S., Swerdlow, R. H., and Oliveira, C. R. (2001) Functional mitochondria are required for amyloid β-mediated neurotoxicity. *FASEB J.* **15,** 1439–1441
13. Devi, L., Prabhu, B. M., Galati, D. F., Avadhani, N. G., and Anandatheerthavarada, H. K. (2006) Accumulation of amyloid precursor protein in the mitochondrial import channels of human Alzheimer's disease brain is associated with mitochondrial dysfunction. *J. Neurosci.* **26,** 9057–9068
14. Hansson, C. A., Frykman, S., Farmery, M. R., Tjernberg, L. O., Nilsberth, C., Pursglove, S. E., Ito, A., Winblad, B., Cowburn, R. F., Thyberg, J., and Ankarcrona, M. (2004) Nicastrin, presenilin, APH-1, and PEN-2 form active γ-secretase complexes in mitochondria. *J. Biol. Chem.* **279,** 51654–51660
15. Du, H., Guo, L., Fang, F., Chen, D., Sosunov, A. A., McKhann, G. M., Yan, Y., Wang, C., Zhang, H., Molkentin, J. D., Gunn-Moore, F. J., Vonsattel, J. P., Arancio, O., Chen, J. X., and Yan, S. D. (2008) Cyclophilin D deficiency attenuates mitochondrial and neuronal perturbation and ameliorates learning and memory in Alzheimer's disease. *Nat. Med.* **14,** 1097–1105
16. Jin, J., Hulette, C., Wang, Y., Zhang, T., Pan, C., Wadhwa, R., and Zhang, J. (2006) Proteomic identification of a stress protein, mortalin/mthsp70/GRP75: relevance to Parkinson disease. *Mol. Cell Proteomics* **5,** 1193–1204
17. Sakahira, H., Breuer, P., Hayer-Hartl, M. K., and Hartl, F. U. (2002) Molecular chaperones as modulators of polyglutamine protein aggregation and toxicity. *Proc. Natl. Acad. Sci. U.S.A.* **99,** 16412–16418
18. Dou, F., Netzer, W. J., Tanemura, K., Li, F., Hartl, F. U., Takashima, A., Gouras, G. K., Greengard, P., and Xu, H. (2003) Chaperones increase association of tau protein with microtubules. *Proc. Natl. Acad. Sci. U.S.A.* **100,** 721–726
19. Gupta, R. S., Ramachandra, N. B., Bowes, T., and Singh, B. (2008) Unusual cellular disposition of the mitochondrial molecular chaperones Hsp60, Hsp70 and Hsp10. *Novartis Found Symp.* **291,** 59–68; discussion 69–73, 137–140
20. Sanjuán Szklarz, L. K., Guiard, B., Rissler, M., Wiedemann, N., Kozjak, V., van der Laan, M., Lohaus, C., Marcus, K., Meyer, H. E., Chacinska, A., Pfanner, N., and Meisinger, C. (2005) Inactivation of the mitochondrial heat shock protein zim17 leads to aggregation of matrix hsp70s followed by pleiotropic effects on morphology and protein biogenesis. *J. Mol. Biol.* **351,** 206–218
21. Oddo, S., Caccamo, A., Shepherd, J. D., Murphy, M. P., Golde, T. E., Kayed, R., Metherate, R., Mattson, M. P., Akbari, Y., and LaFerla, F. M. (2003) Triple-transgenic model of Alzheimer's disease with plaques and tangles: intracellular Aβ and synaptic dysfunction. *Neuron* **39,** 409–421
22. Snyder, E. Y., Deitcher, D. L., Walsh, C., Arnold-Aldea, S., Hartwieg, E. A., and Cepko, C. L. (1992) Multipotent neural cell lines can engraft and participate in development of mouse cerebellum. *Cell* **68,** 33–51
23. Sultan, A. S., Miyoshi, E., Ihara, Y., Nishikawa, A., Tsukada, Y., and Taniguchi, N. (1997) Bisecting GlcNAc structures act as negative sorting signals for cell surface glycoproteins in forskolin-treated rat hepatoma cells. *J. Biol. Chem.* **272,** 2866–2872
24. Walls, K. C., Ghosh, A. P., Ballestas, M. E., Klocke, B. J., and Roth, K. A. (2009) bcl-2/Adenovirus E1B 19-kd interacting protein 3 (BNIP3) regulates hypoxia-induced neural precursor cell death. *J. Neuropathol. Exp. Neurol.* **68,** 1326–1338
25. Walls, K. C., Ghosh, A. P., Franklin, A. V., Klocke, B. J., Ballestas, M., Shacka, J. J., Zhang, J., and Roth, K. A. (2010) Lysosome dysfunction triggers Atg7-dependent neural apoptosis. *J. Biol. Chem.* **285,** 10497–10507
26. Freude, K. K., Penjwini, M., Davis, J. L., LaFerla, F. M., and Blurton-Jones, M. (2011) Soluble amyloid precursor protein induces rapid neural differentiation of human embryonic stem cells. *J. Biol. Chem.* **286,** 24264-24274
27. Kayed, R., Head, E., Sarsoza, F., Saing, T., Cotman, C. W., Necula, M., Margol, L., Wu, J., Breydo, L., Thompson, J. L., Rasool, S., Gurlo, T., Butler, P., and Glabe, C. G. (2007) Fibril specific, conformation dependent antibodies recognize a generic epitope common to amyloid fibrils and fibrillar oligomers that is absent in prefibrillar oligomers. *Mol. Neurodegener.* **2,** 18
28. Blass, J. P., Sheu, R. K., and Gibson, G. E. (2000) Inherent abnormalities in energy metabolism in Alzheimer disease. Interaction with cerebrovascular compromise. *Ann. N.Y. Acad. Sci.* **903,** 204–221
29. Rhein, V., Song, X., Wiesner, A., Ittner, L. M., Baysang, G., Meier, F., Ozmen, L., Bluethmann, H., Dröse, S., Brandt, U., Savaskan, E., Czech, C., Götz, J., and Eckert, A. (2009) Amyloid-β and tau synergistically impair the oxidative phosphorylation system in triple transgenic Alzheimer's disease mice. *Proc. Natl. Acad. Sci. U.S.A.* **106,** 20057–20062
30. Winton, M. J., Lee, E. B., Sun, E., Wong, M. M., Leight, S., Zhang, B., Trojanowski, J. Q., and Lee, V. M. (2011) Intraneuronal APP, not free Aβ peptides in 3xTg-AD mice: implications for tau versus Aβ-mediated Alzheimer neurodegeneration. *J. Neurosci.* **31,** 7691–7699
31. Gupta, R. S. (1990) Mitochondria, molecular chaperone proteins and the *in vivo* assembly of microtubules. *Trends Biochem. Sci.* **15,** 415–418
32. Devi, L., and Ohno, M. (2011) Mitochondrial dysfunction and accumulation of the beta-secretase-cleaved C-terminal fragment of APP in Alzheimer's disease transgenic mice. *Neurobiol. Dis.* **45,** 417–424
33. Yang, T. T., Hsu, C. T., and Kuo, Y. M. (2009) Amyloid precursor protein, heat-shock proteins, and Bcl-2 form a complex in mitochondria and modulate mitochondria function and apoptosis in N2a cells. *Mech. Ageing Dev.* **130,** 592–601
34. Kaden, D., Voigt, P., Munter, L. M., Bobowski, K. D., Schaefer, M., and Multhaup, G. (2009) Subcellular localization and dimerization of APLP1 are strikingly different from APP and APLP2. *J. Cell Sci.* **122,** 368–377
35. Chandra, D., Choy, G., and Tang, D. G. (2007) Cytosolic accumulation of HSP60 during apoptosis with or without apparent mitochondrial release: evidence that its pro-apoptotic or pro-survival functions involve differential interactions with caspase-3. *J. Biol. Chem.* **282,** 31289–31301
36. Xanthoudakis, S., Roy, S., Rasper, D., Hennessey, T., Aubin, Y., Cassady, R., Tawa, P., Ruel, R., Rosen, A., and Nicholson, D. W. (1999) Hsp60 accelerates the maturation of pro-caspase-3 by upstream activator proteases during apoptosis. *EMBO J.* **18,** 2049–2056
37. Veereshwarayya, V., Kumar, P., Rosen, K. M., Mestril, R., and Querfurth, H. W. (2006) Differential effects of mitochondrial heat shock protein 60 and related molecular chaperones to prevent intracellular β-amyloid-induced inhibition of complex IV and limit apoptosis. *J. Biol. Chem.* **281,** 29468–29478